SCIENTIFIC REP**O**RTS

OPEN

Proteomic analysis reveals an impaired Ca^{2+}/AQP5 pathway in the submandibular gland in hypertension

Jing Zhang[1], Li-Jun Zhong[2], Yang Wang[3], Li-mei Liu[1], Xin Cong[1], Ruo-Lan Xiang[1], Li-Ling Wu[1], Guang-Yan Yu[3] & Yan Zhang[1]

Hypertension is a systemic disorder that affects numerous physiological processes throughout the body. Improper sodium transport is a common comorbidity of hypertension, and sodium transport is also critical for maintaining the secretion of submandibular glands, whether the function of submandibular glands is affected by hypertension remains unclear. To determine whether hypertension induces changes in the protein expression of submandibular glands, we compared the proteome of submandibular glands from 14-week-old spontaneously hypertensive rats (SHR) and Wistar Kyoto (WKY) rats using LC-MS/MS. The results revealed that 95 proteins displayed different levels of expression between the submandibular glands from the SHRs and WKYs. Among these, 35 proteins were more abundant, and 60 proteins were less abundant in the SHR compared with the WKY rats. Specifically, aquaporin 5 and parvalbumin, which are correlated with water transport and intracellular Ca^{2+} signal transduction, were verified to exhibit differences in protein abundance. Impaired Ca^{2+} response to carbachol was confirmed in the acinar cells from SHRs, and hyposecretion by the submandibular glands was further confirmed by *in vivo* saliva collection. In conclusion, the proteomic analysis of the submandibular glands of SHRs revealed novel changes in protein abundance that provides possible mechanisms connecting hypertension and hyposecretion in submandibular glands.

Hypertension, also known as high blood pressure, is a long-term systemic disorder that affects numerous physiological processes throughout the body. Although many theories have been proposed to understand the pathogenesis and etiology of hypertension, in many cases, the detailed pathophysiology remain largely unknown[1]. Essential hypertension may be the result of increased sympathetic drive, a nonspecific increased response to norepinephrine, or abnormal cellular cation metabolism; specifically, Na$^+$ imbalance may play a role in the structural reinforcement of hypertension[2]. Na$^+$ reabsorption is enhanced in rats with various forms of experimental and genetic hypertension[3–5]. Moreover, Na$^+$ transport plays an important role in regulating salivation[6]. Whether saliva production is affected by hypertension remains controversial. Elevated blood pressure has been reported to be associated with decreased salivary flow[7–10]. The infusion of angiotensin II into the parotid gland via the carotid artery causes a substantial reduction in the saliva secretion rate, which suggests a direct inhibitory effect of angiotensin II on the parotid that is possibly mediated by a constricting action on its vasculature or alters in water and electrolyte transport[11]. However, there are contradictory reports that have stated that there is no clear physiologic reason to suggest that hypertension should influence salivary function[12,13]. Therefore, whether hypertension affects salivation needs to be clarified.

The spontaneously hypertensive rat (SHR) is the most widely used animal model of essential hypertension and its accompanying metabolic disturbances when under special environmental conditions (for example, when fed a high-fructose or folate-deficient diet)[14]. Age-matched Wistar-Kyoto (WKY) rats are used as controls in most

[1]Department of Physiology and Pathophysiology, Peking University Health Science Center and Key Laboratory of Molecular Cardiovascular Sciences, Ministry of Education, Beijing, China. [2]Medical and Health Analysis Center, Peking University Health Science Center, Beijing, China. [3]Department of Oral and Maxillofacial Surgery, Peking University School and Hospital of Stomatology, Beijing, China. Jing Zhang and Li-Jun Zhong contributed equally to this work. Correspondence and requests for materials should be addressed to Y.Z. (email: zhangy18@bjmu.edu.cn)
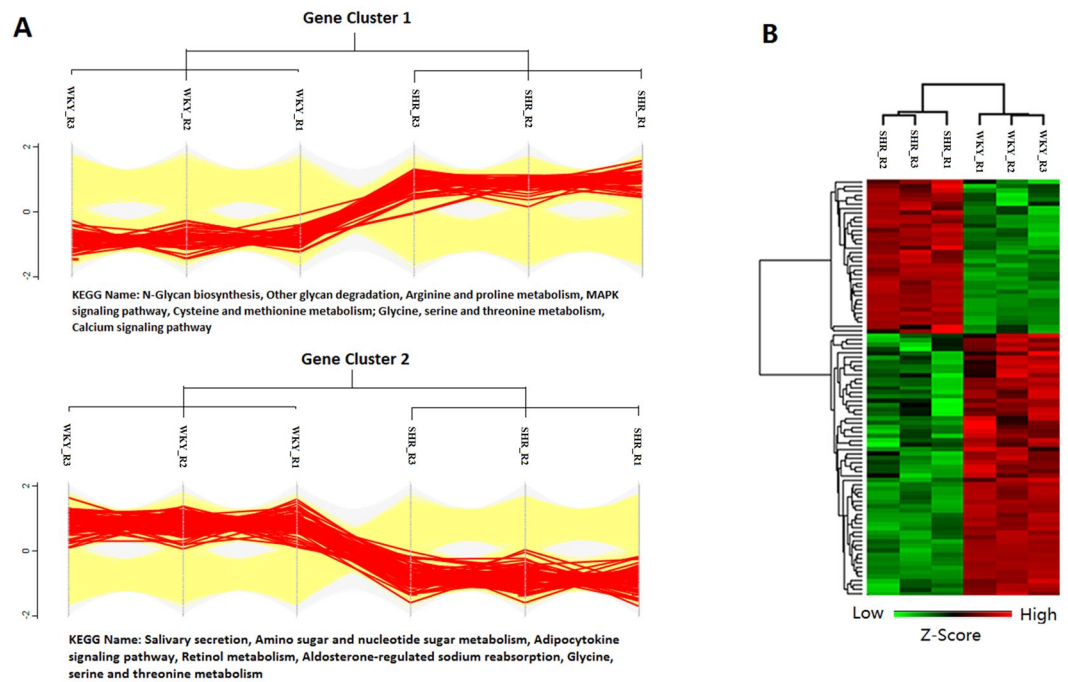
Figure 1. Analysis of the differentially expressed proteins. (**A**) Profile plot of the 95 differentially expressed proteins in 3 samples from each group. Categorical annotation in the form of participation in a KEGG pathway is supplied under the plot. (**B**) Hierarchical clustering analysis of the 95 significantly differentially expressed proteins. Red represents a high z-score, and green represents a low z-score.

studies. Currently, the molecular changes that salivary glands undergo in chronic essential hypertension are not fully established.

The aim of this study was to apply a proteomic approach to identify altered proteins and pathways involved in salivation in the submandibular glands (SMGs) of SHRs compared with those in WKY. The results revealed altered protein abundances in the glands of the SHRs. We further confirmed an impaired Ca^{2+} signal, a reduced abundance of AQP5, and hyposecretion in the SHR SMGs.

Results

Protein expression analysis.   Scatter plots of the log2-fold changes (X) and log10 *P* values (Y) revealed the proteome expression profiles of the two groups (Supplemental Fig. 1A). The red dots represent proteins that were up-regulated in the SHR group, and the green dots represent down-regulated proteins. The Venn diagrams represent the numbers of proteins that were identified in each of three biological replicates (Supplemental Fig. 1B). A total of 4619 proteins were identified in all three biological replicates using the shotgun method, and 4329 of these proteins were quantified with a label-free algorithm (at least 2 peptides of a protein were repeatedly measured in at least three samples). We found a total of 95 significantly differentially expressed proteins, among which 35 were up-regulated and 60 were down-regulated in the SHR group. To select the proteins that were differentially expressed in the SHR group, fold-changes greater than 2 and *P* values below 0.05 (using Student's t-test) were used as the criteria. A profile plot of the differentially expressed proteins with categorical annotation (Fig. 1A) revealed that the up-regulated proteins in the SHR group were involved in the KEGG pathway of N-glycan biosynthesis, arginine and proline metabolism, a MAPK signaling pathway, cysteine and methionine metabolism, glycine, serine and threonine metabolism, and calcium signaling pathways, whereas the down-regulated proteins were involved in salivary secretion, amino sugar and nucleotide sugar metabolism, the adipocytokine signaling pathway, retinol metabolism, aldosterone-regulated sodium reabsorption, and glycine, serine and threonine metabolism. Hierarchical clustering analysis was performed to visualize the 95 significantly differentially expressed proteins between SHRs and WKYs. Red means up-regulated proteins and green means down-regulated proteins in SHR (Fig. 1B). The details for the top 10 proteins that were more or less abundant in the SHRs compared with the WKYs are listed in Table 1.

Decreased expression and membrane distribution of AQP5 in the SMGs of the SHRs.   Target proteins were chosen upon evaluation of the proteomics analysis (i.e., differential quantitation) and through consideration of a series of criteria that included protein-protein interaction analysis and the most relevant biological/molecular functions. For this purpose, one up-regulated protein (parvalbumin) and one down-regulated protein (AQP5) were chosen. Western blotting confirmed that AQP5 was obviously reduced in the SHR group compared with the WKY group (Fig. 2A). Immunofluorescent analysis revealed that AQP5 was mainly localized to the apical and lateral plasma membranes of the acinar cells in the WKY SMGs. In the SMGs of the SHRs, AQP5 staining in the acini was markedly declined, but the distribution still limited to the apical and lateral plasma membranes (Fig. 2B).

Accession	Gene	Protein	Fold change	—log P value
Less abundant in SHR				
P47864	Aqp5	Aquaporin-5	0.092867715	3.13868
D4AED6	RGD1307782	Williams-Beuren syndrome critical region protein 27	0.095108757	2.89472
M0RE00	Tbca	Tubulin-specific chaperone A	0.12963352	3.46293
Q63550	Bpifa2f	BPI fold containing family A, member 2 F	0.159751431	3.09471
G3V709	Naprt1	Nicotinate phosphoribosyltransferase	0.167758024	4.62788
P48450	Lss	Lanosterol synthase	0.189945151	4.40373
D4AAB9	Paip2b	Poly(A) binding protein interacting protein 2B	0.201330033	1.55368
Q5PQP2	Ebag9	Receptor-binding cancer antigen expressed on SiSo cells	0.224552021	1.66317
D3ZN19	Rnf121	Ring finger protein 121	0.231378992	1.91671
Q99JC6	Tapbp	TAP binding protein	0.232509528	3.3854
More abundant in SHR				
P02625	Pvalb	Parvalbumin alpha	2.441750094	3.11535
P08733	Myl2	Myosin regulatory light chain 2, ventricular/cardiac muscle isoform	2.573624401	1.57846
G3V885	Myh6	Myosin-6	3.018308012	3.51078
Q66H40	Hmgn3	High mobility group nucleosome-binding domain-containing protein 3	3.033480339	1.93548
Q4PP99	Tnnc1	Troponin C type 1	3.082486958	2.58497
O09171	Bhmt	Betaine–homocysteine S-methyltransferase 1	3.765760717	5.04722
P47727	Cbr1	Carbonyl reductase 1	3.773230395	5.12838
P13601	Aldh1a7	Aldehyde dehydrogenase, cytosolic 1	5.507811394	3.67567
D4A0S3	Grpcb	Glutamine/glutamic acid-rich protein A	5.534638554	3.47886
Q9QZ76	Mb	Myoglobin	6.765551592	3.61407

Table 1. Top 10 proteins more or less abundant in SHR compared with WKY.

Impaired calcium signaling in the SMGs of the SHRs. Western blotting confirmed that parvalbumin protein expression was obviously reduced in the SHR group compared with the WKY group (Fig. 3A). Since parvalbumin acts as a Ca^{2+}-binding protein and plays a role in Ca^{2+} homeostasis in many types of cells, whether the up-regulated parvalbumin altered the Ca^{2+} signal in the SMG needed to be studied. To clarify whether $[Ca^{2+}]_i$ mobilization changed in the SHRs compared with the WKYs, we measured the $[Ca^{2+}]_i$ in isolated SMG acinar cells in response to $10\,\mu mol/L$ carbachol, which is an agonist of muscarinic receptors. The peak Ca^{2+} responses to carbachol and responses at 50 s after stimulation were much smaller in the SHRs than in the WKYs (Fig. 3B).

Fluid secretion from the SMGs decreased in the SHR rats. To investigate whether secretion by the SMGs was affected in the SHRs, *in vivo* saliva collection was performed from the SHR rats, and the WKY rats served as controls. The flow rates and total volumes of secreted saliva were measured in response to $10\,\mu g/g$ pilocarpine. The total amount of saliva secreted in 10 min was decreased by 47.4% in the SHRs (Fig. 4A). The secretion rate was relatively constant but slower during the entire 10 min stimulation period in the SHR rats compared with the WKY controls (Fig. 4B). The *in vivo* saliva collections from the SMGs suggested impaired salivation in the SHR rats.

Discussion

In the present study, we investigated the extent to which hypertension affected SMG protein expression and salivation. In total, 95 proteins exhibited expressions that were altered by over 2 fold in the SHR compared to the WKY rats. Furthermore, we demonstrated that secretion from the SMGs was decreased in the SHR rats. The mechanism included not only the down-regulated expression of AQP5 but also an impaired Ca^{2+} signal in the acinar cells. Accordingly, these results provide new insights into how hypertension may affect secretion from SMGs through alterations in the glands' proteomes.

Clinical studies have reported that hypertension decreases saliva secretion in patients[7,9,10]. However, these studies have been challenged by other researchers who have found no obvious change in the flow rate in conditions of hypertension but have rather found potential pH changes[15]. Therefore, well-designed experiments are required to precisely investigate the effects of hypertension on salivary flow. Here, we conducted a proteomic investigation of the effects of hypertension on the SMG with the aim of identifying a possibly altered protein expression pattern in SHRs compared with WKYs using the techniques of LC/MS/MS. We found a total of 95 proteins with altered abundances in the hypertension group, and two of these that have been reported to be directly involved in the regulation of salivation were validated in subsequent experiments. The functions of the remaining 93 proteins need to be studied in the future.

AQP5 is well-known to be enriched in salivary glands, and in these glands, AQP5 is mainly localized in the apical membrane of the acinar cells and plays an important role in transepithelial water transport from the interstitium to the acinar lumen[16]. Proper expression and correct subcellular localization of AQP5 are required in maintaining salivary gland function[17-19]. Parasympathetic innervation is essential for the expression and distribution of AQP5 in the salivary gland[20-22]. In this study, we observed that AQP5 was localized to the apical
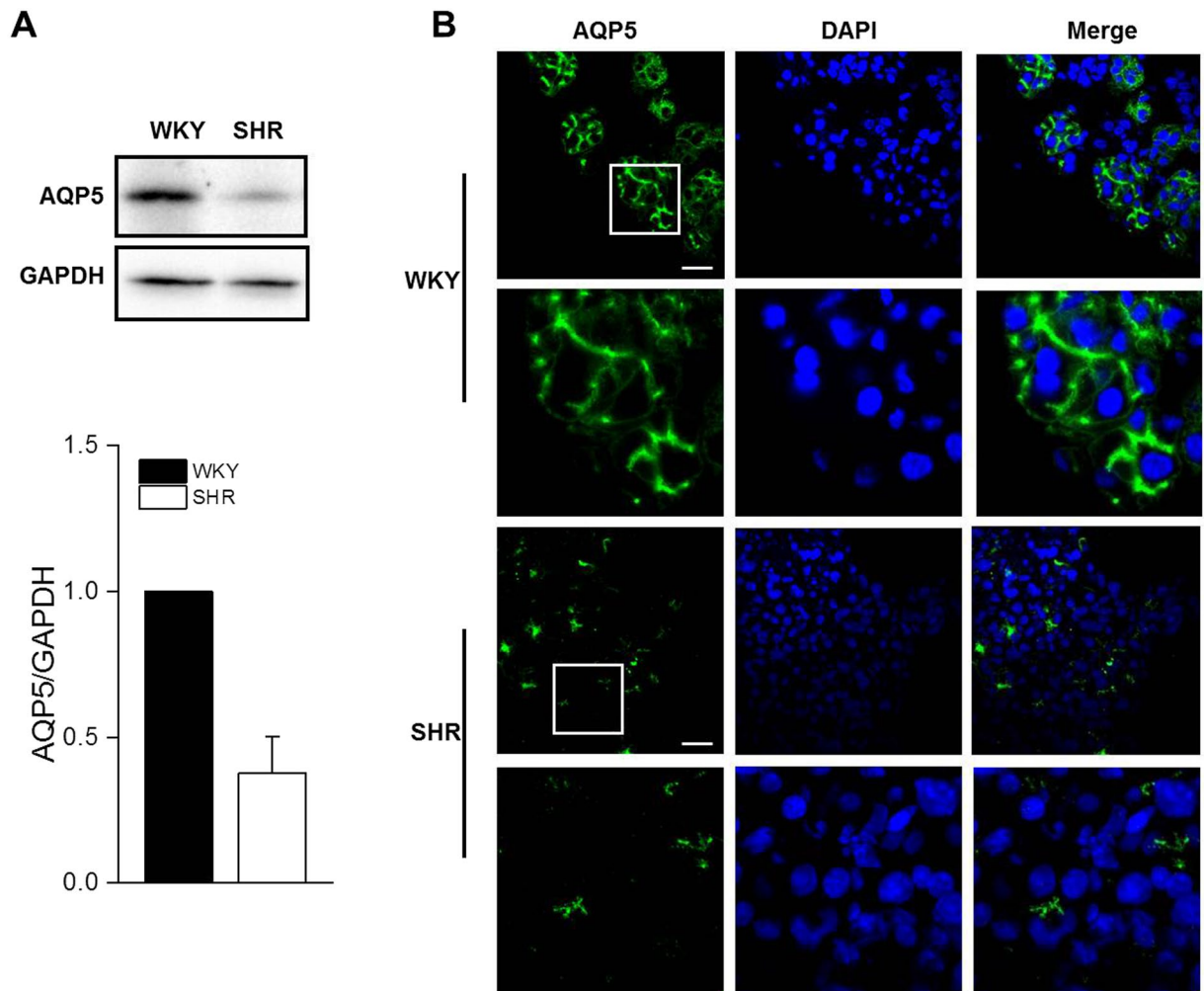
Figure 2. Decreased expression and membrane distribution of AQP5 in the SMGs of the SHRs. (**A**) Western blot analyses and (**B**) immunofluorescent staining for AQP5 in the submandibular glands of the SHR and WKY rats. The values are mean ± S.E.M. of four animals. **$P < 0.01$ vs. WKY. Scale bars: 30 μm. The displayed blots are cropped blots, and full-length blots are presented in Supplementary Figures 2 and 3.

and lateral plasma membranes of the acinar cells in the control SMGs, which is consistent with previous studies. However, in the SHR SMGs, AQP5 expression was dramatically decreased, and this decrease was among the most substantial in the proteomic analysis, which was validated using Western blot. The immunofluorescent results revealed that the staining pattern from the SHRs appeared similar to that from the WKYs. These results suggest that hypertension may decrease salivary secretion by directly down-regulating the expression of AQP5 without affecting its distribution.

Parvalbumins are acidic, intracellular Ca^{2+}-binding proteins of low molecular weight. They are associated with several Ca^{2+}-mediated cellular activities and physiological processes[23]. It has been suggested that parvalbumin might function as a "Ca^{2+} shuttle" that transports Ca^{2+} from troponin-C to the sarcoplasmic reticulum Ca^{2+} pump during muscle relaxation in muscle cells, which makes parvalbumin the most important soluble protein for Ca^{2+} buffering[24]. The overexpression of parvalbumin has been demonstrated to facilitate myocardial relaxation both *in vitro* and *in vivo*[25]. The transfer of the parvalbumin gene into normal and diseased cardiac myocytes increases the relaxation rate but also markedly decreases the contraction amplitude[26]. Together, these results suggest that parvalbumin acts as a unique "delayed" Ca^{2+} buffer and facilitates Ca^{2+} sequestration from the cytosol. Additionally, the expression of parvalbumin is up-regulated in $AQP4^{-/-}$ mice, which suggests that AQP4 affects intracellular Ca^{2+} dynamics by changing the expression of proteins involved in Ca^{2+} buffering[27]. In our results, the proteomic analysis revealed that parvalbumin was up-regulated in the SHR group, and this result was also validated by Western blot. Since the up-regulation of parvalbumin suggests a delayed Ca^{2+} signal in the SMG cells. We further detect the Ca^{2+} response to carbachol in isolated acinar cells from the SHR group, and the results demonstrated that the Ca^{2+} signal was impaired not only at the peak but also throughout the whole procedure when compared with the Ca^{2+} signal in the acinar cells of the WKYs. Whether parvalbumin was induced by impaired AQP5 in the SHRs is still unknown and requires further study.

In conclusion, our data demonstrated that protein abundances were significantly changed in the SMGs from the SHRs compared with the glands from the WKY rats. Among the proteins that were altered, AQP5 and
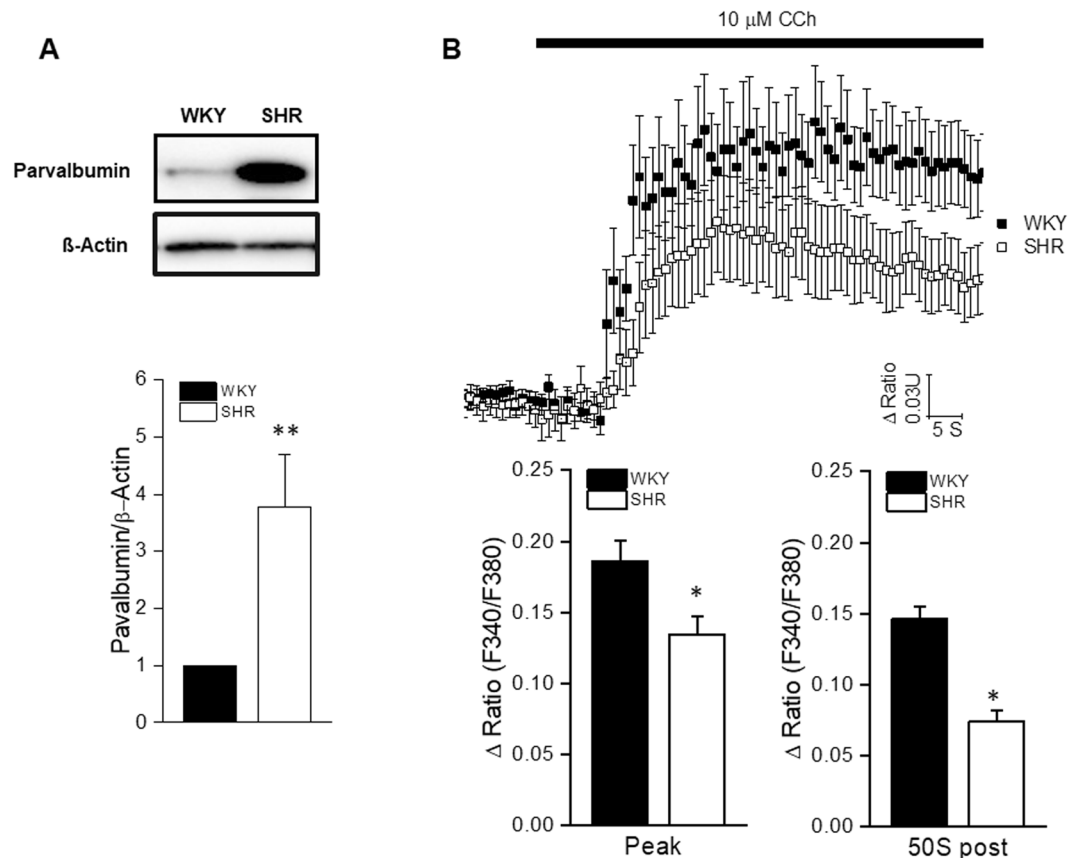
Figure 3. Impaired Ca^{2+} signaling in the SMGs of the SHRs. (**A**) Western blot analyses of parvalbumin in the submandibular glands of the SHR and WKY rats. The values are mean $\pm$ S.E.M. **$P < 0.01$ vs. WKY. The displayed blots are cropped blots, and full-length blots are presented in Supplementary Figures 4 and 5. (**B**) Acinar cells were loaded with fura-2 AM to determine the intracellular Ca^{2+} levels and were stimulated with $10\,\mu mol/L$ carbachol during the indicated time. The magnitudes of the Ca^{2+} responses to carbachol at the peak and 50 s after stimulation are presented. The values are mean $\pm$ S.E.M. of 48 cells from six animals. *$P < 0.05$ vs. WKY.

parvalbumin were among those that exhibited the greatest changes in the proteomic analysis and were further validated. Secretion from the SMGs was obviously decreased in the SHR group. The underlying mechanisms of hyposecretion by the SMGs include not only the sequestration of Ca^{2+} from the cytosol by up-regulated parvalbumin but also the decreased expression of AQP5 in the glands. These findings improve our understanding of the mechanism by which hypertension suppresses saliva secretion and may provide new insights into future therapeutics for treating hypertension.

Materials and Methods

Animals. Male SHR (14 weeks old, early hypertension) and WKY (14 weeks old, normotension) rats were used in compliance with the Institutional Authority for Laboratory Animal Care of the Peking University Health Science Center, China. All experimental procedures were approved by the Ethics Committee for Animal Research of Peking University Health Science Center and complied with the Guide for the Care and Use of Laboratory Animals (NIH Publication No. 8523, revised 1996). A total of 16 rats in each group were used in this study. 6 rats were used in Ca^{2+} imaging, 6 rats were used in saliva collection, and 4 were used for Western blot, proteomic analysis, and immunofluorescence. The SMGs were carefully removed from the anesthetized rats and snap frozen in liquid nitrogen followed by storage at $-80\,°C$.

Chemicals. Ammonium bicarbonate, sodium deoxycholate, iodoacetamide, dithiothreitol, and all mobile phases and solutions prepared with HPLC grade solvents (i.e. water, acetonitrile, methanol, and formic acid) were purchased from Sigma (St. Louis, MO, USA). Tris-(2-carboxyethyl) phosphine was acquired from Thermo Scientific (Rockford, IL, USA). Modified sequencing-grade trypsin was obtained from Promega (Madison, WI, USA).

Protein digestion and peptide fractionation. Crude protein was isolated from the SMGs and quantified as described previously[28]. The protein samples were digested according to the manufacturer's protocol for filter-aided sample preparation[29]. The peptides were separated with high-pH reversed-phase chromatography using a Dionex Ultimate 3000 Micro Binary HPLC pump system[30]. The eluted peptides were pooled as 15 fractions and vacuum-dried. Next, the samples were ready for nano-ESI-LC-MS/MS analysis.
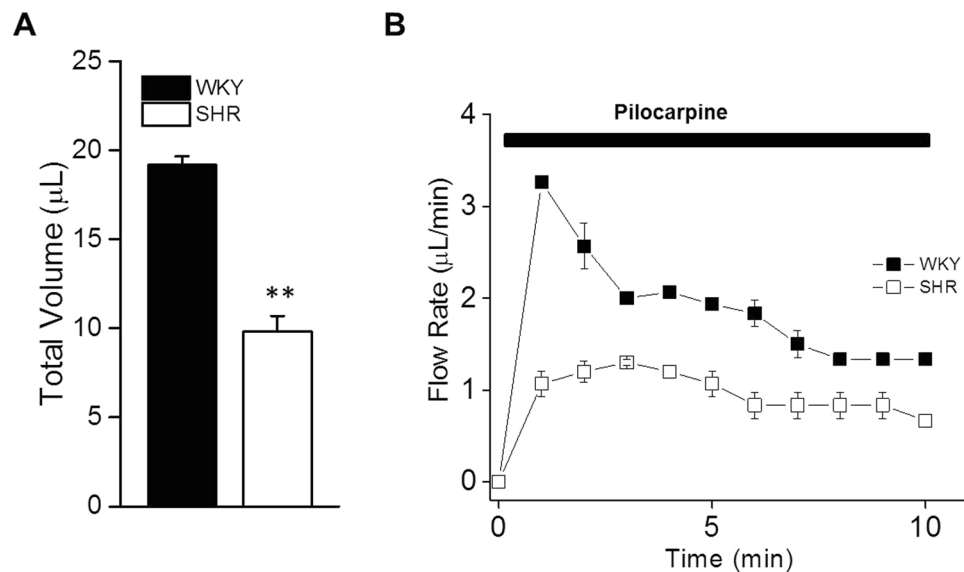
Figure 4. Changes in agonist-induced fluid secretion in the SHR and WKY rats. *In vivo* saliva collected from submandibular glands stimulated with pilocarpine ($10 \mu g/g$, i.p.). (**A**) The total volume ($\mu l/10 \min$) and (**B**) flow rate ($\mu l/\min$) were decreased in the SHRs compared with the WKYs. The values are mean $\pm$ S.E.M. of six animals. $**P < 0.01$ vs. WKY.

LC-MS/MS and Label-Free Quantification.   The analysis was performed in triplicate on a nano-flow HPLC system connected to a LTQ-Orbitrap Velos Pro mass spectrometer equipped with a Nanospray Flex Ion Source (Thermo Fisher Scientific, Waltham, MA, USA). Briefly, the peptides were separated in a pre-column (Easy-column C18-A1, $100 \mu m$ I.D.$\times 20$ mm, $5 \mu m$) and a reversed phase C18 column (Easy-column C18-A2, $75 \mu m$ I.D. $\times 100$ mm, $3 \mu m$). The eluting peptides were ionized with an electrospray maintained at 2.2 kV, and the 15 most abundant ions detected in the full-MS scan were measured in the LTQ part by collision-induced dissociation. Each group was analyzed in three biological replicates. The raw data analyses were performed with MaxQuant software (version1.4.1.2, http://www.maxquant.org/). For protein identification, the MS/MS data were submitted to the Uniprot human protein database (release 3.43, 72,340 sequences).

Label-free quantitation (LFQ) was also performed in MaxQuant. The minimum ratio count for the LFQ was set to 2, and the match-between-runs option was enabled. The other parameters were set to the defaults. The up-regulated and down-regulated proteins were defined as those with significantly altered protein ratios and *P* values. The significance of the *P* values was calculated with the Perseus software (version 1.4.1.3, http://www.perseus-framework.org/).

Bioinformatics Analysis.   The protein expression analyses were performed with the Perseus software. Scatter plots were constructed with the log2-fold change (X) and log10 *P* value (Y). For the hierarchical clustering analysis of the differentially expressed proteins, the LFQ intensity of each protein was processed by a log2(x) transformation, and the Z-score was then calculated. The color of the bar represents the Z-score of each protein. The profile plot of the differentially expressed proteins was created with categorical annotation supplied in the form of the participation in a KEGG pathway. All annotations were extracted from the UniProt database. The Venn diagrams revealed the numbers of proteins identified in each of the three biological replicates.

Proteomic validation by Western blotting.   The proteins ($40 \mu g$) were separated on 12% SDS-PAGE gels, transferred to polyvinylidene difluoride membranes, blocked with 5% non-fat milk, probed with primary antibodies against aquaporin 5 (AQP5) (Santa Cruz Biotechnology, CA, USA) and parvalbumin (Abcam, Cambridge, MA, USA) at $4 \,^{\circ}C$ overnight, and incubated with horseradish peroxidase-conjugated secondary antibodies. The immunoreactive bands were then visualized by enhanced chemiluminescence. ß-actin (Santa Cruz Biotechnology, CA, USA) and GAPDH (Abcam, Cambridge, MA, USA) was used as a loading control.

Immunofluorescence.   The glands were taken from $-80 \,^{\circ}C$, embedded into OCT and cut into $5 \mu m$ sections. Frozen sections were fixed in cold acetone for 15 min, blocked with 10% goat serum, immunostained with primary antibodies against AQP5 (1:100) overnight at $4 \,^{\circ}C$ followed by an Alex 488-labeled secondary antibody. The nuclei were stained with 4,6-diamidino-2-phenylindole (Sigma, St. Louis, MO, USA). The fluorescence images were captured by confocal microscopy (Olympus FV1200, Japan).

Ca^{2+} Imaging.   SMG acinar cells were prepared by enzyme digestion as previously reported with minor modification[31]. In brief, the rats were euthanized, and the glands were dissected, finely minced, digested in minimal essential medium (MEM, Invitrogen, Grand Island, NY, USA) containing 1% bovine serum albumin and

0.125 mg/ml Liberase TL enzyme (Roche Applied Science, Indianapolis, IN, USA) for 25 min at 37 °C, and then centrifuged. The cell pellet was resuspended and digested in Liberase TL for another 25 min. Following digestion, the cells were rinsed in MEM supplemented with 1% BSA.

The fura-2 fluorescence ratiometric method was used to measure the intracellular free calcium levels. The cells were loaded with 2 μM fura-2/AM for 25 min at room temperature. Imaging was performed using an inverted microscope (IX71, Olympus, Japan) equipped with a Polychrome IV Imaging System coupled to a high-speed digital camera (Till Photonics, Pleasanton, CA, USA). Images from the fura-2 (Invitrogen, Grand Island, NY, USA)-loaded cells were acquired every second for carbachol (Sigma, St. Louis, MO, USA) by alternate excitation with light at 340 nm and 380 nm, and emission was captured at 510 nm using MetaFluor7.0 (Molecular Devices, Sunnyvale, CA, USA). The chamber volume was maintained at ~100 μl. The fluorescence ratio of 340 nm over 380 nm was calculated, and all data are presented as the change in ratio units.

Measurement of stimulated salivary flow.   The rats were fasted for a minimum of 5 h with water provided ad libitum. The saliva secreted from the SMGs was collected for 10 min from surgically isolated ducts using a micropipette starting 5 min after pilocarpine (Abcam, Cambridge, MA, USA) injection (10 μg/g body weight, i.p.) under anesthesia. The volume of saliva was measured, and the salivary flow rate is represented as microliters per minute.

Statistics.   The data are expressed as mean ± S.E.M. The statistical analyses were performed using one-way ANOVA followed by Bonferroni's test for multiple comparisons with Origin 2016 software (OriginLab, MA, USA). Differences were considered statistically significant at $P < 0.05$. For the discovery stage, a 2-fold change and a Student's t-test P value of 0.05 were used as combined thresholds to define the biologically regulated proteins.

References

1. Bie, P. & Evans, R. G. Normotension, hypertension and body fluid regulation: Brain and kidney. *Acta physiologica*, https://doi.org/10.1111/apha.12718 (2016).
2. Andersen, L. J., Andersen, J. L., Pump, B. & Bie, P. Natriuresis induced by mild hypernatremia in humans. *American journal of physiology. Regulatory, integrative and comparativephysiology* **282**, R1754–1761, https://doi.org/10.1152/ajpregu.00732.2001 (2002).
3. Heidland, A., Rockel, A. & Schmid, G. Salivary kallikrein excretion in hypertension. *Klinische Wochenschrift* **57**, 1047–1052 (1979).
4. Wotman, S., Mandel, I. D., Thompson, R. H. Jr & Laragh, J. H. Salivary electrolytes, urea nitrogen, uric acid and salt taste thresholds in hypertension. *Journal of oral therapeutics and pharmacology* **3**, 239–250 (1967).
5. Adlin, V., Channick, B. J. & Marks, A. D. Salivary sodium-potassium ratio and plasma renin activity in hypertension. *Circulation* **39**, 685–692 (1969).
6. Kopach, O. *et al*. Cannabinoid receptors in submandibular acinar cells: functional coupling between saliva fluid and electrolytes secretion and Ca2 + signalling. *Journal of cell science* **125**, 1884–1895, https://doi.org/10.1242/jcs.088930 (2012).
7. Bohm, R., van Baak, M., van Hooff, M., Moy, J. & Rahn, K. H. Salivary flow in borderline hypertension. *Klinische Wochenschrift* **63 Suppl 3**, 154–156 (1985).
8. van Hooff, M., van Baak, M. A., Schols, M. & Rahn, K. H. Studies of salivary flow in borderline hypertension: effects of drugs acting on structures innervated by the autonomic nervous system. *Clinical science* **66**, 599–604 (1984).
9. Rahn, K. H., van Baak, M., van Hooff, M. & Schols, M. Studies on salivary flow in borderline hypertension. *Journal of hypertension. Supplement: official journal of the International Society of Hypertension* **1**, 77–78 (1983).
10. Labat, C. *et al*. Inflammatory mediators in saliva associated with arterial stiffness and subclinical atherosclerosis. *Journal of hypertension* **31**, 2251–2258, https://doi.org/10.1097/HJH.0b013e328363dccc discussion2258 (2013).
11. McKinley, M. J., Denton, D. A., Hatzikostas, S. & Weisinger, R. S. Effect of angiotensin II on parotid saliva secretion in conscious sheep. *The American journal of physiology* **237**, E56–60 (1979).
12. Streckfus, C. F., Wu, A. J., Ship, J. A. & Brown, L. J. Stimulated parotid salivary flow rates in normotensive, hypertensive, and hydrochlorothiazide-medicated. *Journal of oral pathology & medicine: official publication of the International Association of Oral Pathologists and the American Academy of Oral Pathology* **23**, 280–283 (1994).
13. Streckfus, C. F., Wu, A. J., Ship, J. A. & Brown, L. J. Comparison of stimulated parotid salivary gland flow rates in normotensive and hypertensive persons. *Oral surgery, oral medicine, and oral pathology* **77**, 615-619 (1994).
14. Pravenec, M. Use of rat genomics for investigating the metabolic syndrome. *Methods in molecular biology* **597**, 415–426, https://doi.org/10.1007/978-1-60327-389-3_28 (2010).
15. Kagawa, R. *et al*. Influence of hypertension on pH of saliva in older adults. *Oral diseases* **19**, 525–529, https://doi.org/10.1111/odi.12043 (2013).
16. Matsuzaki, T. *et al*. Function of the membrane water channel aquaporin-5 in the salivary gland. *Acta histochemica et cytochemica* **45**, 251–259, https://doi.org/10.1267/ahc.12018 (2012).
17. Krane, C. M. *et al*. Salivary acinar cells from aquaporin 5-deficient mice have decreased membrane water permeability and altered cell volume regulation. *The Journal of biological chemistry* **276**, 23413–23420, https://doi.org/10.1074/jbc.M008760200 (2001).
18. Satoh, K. *et al*. E2f1-deficient NOD/SCID mice have dry mouth due to a change of acinar/duct structure and the down-regulation of AQP5 in the salivary gland. *Pflugers Archiv: European journal of physiology* **465**, 271–281, https://doi.org/10.1007/s00424-012-1183-y (2013).
19. Mizumachi-Kubono, M., Watari, I., Ishida, Y. & Ono, T. Unilateral maxillary molar extraction influences AQP5 expression and distribution in the rat submandibular salivary gland. *Archives of oral biology* **57**, 877–883, https://doi.org/10.1016/j.archoralbio.2012.02.006 (2012).
20. Ishikawa, Y., Eguchi, T., Skowronski, M. T. & Ishida, H. Acetylcholine acts on M3 muscarinic receptors and induces the translocation of aquaporin5 water channel via cytosolic Ca2 + elevation in rat parotid glands. *Biochemical and biophysical research communications* **245**, 835–840, https://doi.org/10.1006/bbrc.1998.8395 (1998).
21. Ishikawa, Y., Inoue, N., Zhenfang, Y. & Nakae, Y. Molecular mechanisms and drug development in aquaporin water channel diseases: the translocation of aquaporin-5 from lipid rafts to the apical plasma membranes of parotid glands of normal rats and the impairment of it in diabetic or aged rats. *Journal of pharmacologicalsciences* **96**, 271–275 (2004).
22. Ishikawa, Y. *et al*. Identification of AQP5 in lipid rafts and its translocation to apical membranes by activation of M3 mAChRs in interlobular ducts of rat parotid gland. *American journal of physiology. Cell physiology* **289**, C1303–1311, https://doi.org/10.1152/ajpcell.00211.2005 (2005).
23. Arif, S. H. A Ca(2 +)-binding protein with numerous roles and uses: parvalbumin in molecular biology and physiology. *BioEssays: news and reviews in molecular, cellular and developmental biology* **31**, 410–421, https://doi.org/10.1002/bies.200800170 (2009).
24. Babu, A., Lehman, W. & Gulati, J. Characterization of the Ca2 + -switch in skeletal and cardiac muscles. *FEBS letters* **251**, 177–182 (1989).

25. Wang, W., Martindale, J. & Metzger, J. M. Parvalbumin: Targeting calcium handling in cardiac diastolic dysfunction. *General physiology andbiophysics* **28 Spec NoFocus**, F3–6 (2009).
26. Asp, M. L., Martindale, J. J., Heinis, F. I., Wang, W. & Metzger, J. M. Calcium mishandling in diastolic dysfunction: mechanisms and potential therapies. *Biochimica et biophysicaacta* **1833**, 895–900, https://doi.org/10.1016/j.bbamcr.2012.09.007 (2013).
27. Basco, D. *et al.* Absence of aquaporin-4 in skeletal muscle alters proteins involved in bioenergetic pathways and calcium handling. *PloS one* **6**, e19225, https://doi.org/10.1371/journal.pone.0019225 (2011).
28. Zhang, Y. *et al.* Expression and characteristics of vanilloid receptor 1 in the rabbit submandibular gland. *Biochemical and biophysical research communications* **345**, 467–473, https://doi.org/10.1016/j.bbrc.2006.04.106 (2006).
29. Wisniewski, J. R., Zougman, A., Nagaraj, N. & Mann, M. Universal sample preparation method for proteome analysis. *Nature methods* **6**, 359-362, https://doi.org/10.1038/nmeth.1322 (2009).
30. Yang, F., Shen, Y., Camp, D. G. 2nd & Smith, R. D. High-pH reversed-phase chromatography with fraction concatenation for 2D proteomic analysis. *Expert review of proteomics* **9**, 129–134, https://doi.org/10.1586/epr.12.15 (2012).
31. Nakamoto, T. *et al.* Purinergic P2X7 receptors mediate ATP-induced saliva secretion by the mouse submandibular gland. *J Biol Chem* **284**, 4815–4822, https://doi.org/10.1074/jbc.M808597200 (2009).

Acknowledgements

Author Contributions

J.Z. and L.J.Z. contributed to the performance of the experiments, data acquisition, analysis, and interpretation, and drafted the manuscript. Y.W. and L.M.L. contributed to the animal experiments and data acquisition. X.C. and R.L.X. contributed to the data acquisition. L.L.W., G.Y.Y., and Y.Z. contributed to the conception and design of this study and critically revised the manuscript.

Additional Information

Supplementary information accompanies this paper at https://doi.org/10.1038/s41598-017-15211-0.

Competing Interests: The authors declare that they have no competing interests.

Publisher's note: Springer Nature remains neutral with regard to jurisdictional claims in published maps and institutional affiliations.